

Hydrodynamic analysis of heavy ion collisions at RHIC

T Hirano

Department of Physics, the University of Tokyo, Tokyo 113-0033, Japan

E-mail: hirano@phys.s.u-tokyo.ac.jp

Abstract. Current status of dynamical modeling of relativistic heavy ion collisions and hydrodynamic description of the quark gluon plasma is reported. We find the hadronic rescattering effect plays an important role in interpretation of mass splitting pattern in the differential elliptic flow data observed at RHIC. To demonstrate this, we predict the elliptic flow parameter for ϕ mesons to directly observe the flow just after hadronisation. We also discuss recent applications of outputs from hydrodynamic calculations to J/ψ suppression, thermal photon radiation and heavy quark diffusion.

1. Introduction

Understanding of the thermodynamic and transport properties of the quark gluon plasma (QGP) is one of the main topics in the physics of relativistic heavy ion collisions [1]. The QGP created in these reactions is by no means a static matter and exists as a transient state whose lifetime is of the order of $\sim 1-10$ fm/ c . It is non-trivial even whether local equilibrium is really reached or not, which should be also clarified through the observation. Hence, one first has to justify the local equilibration by comparing the model calculation with experimental data. This is the starting point of further studies on the QGP under equilibrium. In order to understand thermodynamical (bulk) and transport properties of the QGP in relativistic heavy ion collisions, one then has to develop a *dynamical* analysis tool which links the observables with the equation of state (EoS) and transport coefficients of the QGP. It is inevitable to apply each relevant model to each stage of the collisions and unify these models consistently to describe the whole stage of the reactions.

Along the line of thought, we have constructed a dynamical and unified model based on a fully three-dimensional hydrodynamic description of the QGP [2, 3]. One of the major discoveries at relativistic heavy ion collider (RHIC) is that elliptic flow parameters, which are intimately related with the degree of thermalisation, are well described within a framework of relativistic hydrodynamics [4]. An assumption of local thermalisation has to be made in hydrodynamics. However, local thermalisation can be expected only in the intermediate stage. Thus, one needs to model dynamics of reactions appropriately before and after the hydrodynamic stage to draw informations

of the QGP from experimental data. Once we obtain the hydrodynamic evolution of the QGP, information of local thermodynamic variables is available to analyse other observables such as J/ψ suppression, heavy quark diffusion and thermal radiation. In this way, hydrodynamic models enable one to analyse a vast body of data in relativistic heavy ion collisions.

2. Dynamical modeling of heavy ion collisions

Hydrodynamics is a general framework to describe the space-time evolution of locally thermalised matter for a given EoS. This framework has been applied to the intermediate stage in heavy ion collisions. We neglect the effects of dissipation and concentrate on discussion about ideal hydrodynamic models. The main ingredient in ideal hydrodynamic models is the EoS of hot and dense matter governed by QCD. In addition, one also needs to assign initial conditions to the hydrodynamic equations. Hydrodynamics can be applied to a system as long as its local thermalisation is maintained. However, in the final stage the particles are freely streaming toward the detectors and their mean free path is almost infinite. This is obviously beyond the applicability of hydrodynamics. Hence we also need a description to decouple the particles from the rest of the system. The hydrodynamic modeling of relativistic heavy ion collisions needs an EoS, initial conditions and a decoupling prescription. Hydrodynamic modeling has been sophisticated for these years and tested against RHIC data [4].

The EoS is in principle calculated from lattice QCD simulations. Instead of using the result from lattice QCD simulations, we employ a phenomenological model in this study. At high energy density, the EoS can be described by a bag model

$$P = \frac{1}{3}(e - 4B). \quad (1)$$

Here P is pressure and e is energy density. The bag constant B is tuned to match pressure of the QGP phase to that of a hadron resonance gas at critical temperature T_c : $P_{\text{QGP}}(T_c) = P_{\text{hadron}}(T_c)$. A hadron gas in heavy ion collisions is not in chemical equilibrium below the chemical freezeout temperature T^{ch} which is close to T_c [5], so the hadron phase may not be chemically equilibrated. A chemically frozen (or only partially equilibrated) hadron resonance gas can be described by introducing the chemical potential for each hadron [6, 7].

For a decoupling prescription, the Cooper-Frye formula [8] is almost a unique choice to convert the hydrodynamic picture to the particle picture. Contribution from resonance decays should be taken into account by applying decay kinematics to the outcome of the Cooper-Frye formula. The decoupling temperature T^{dec} is fixed through *simultaneous* fitting of p_T spectra for various hadrons in the low p_T region.

The prescription to calculate the momentum distribution as above is sometimes called the sudden freezeout model since the mean free path of the particles changes from zero (ideal fluid) to infinity (free streaming) within a thin layer. Although this model

is too simple, it has been used in hydrodynamic calculations for a long time. Recently one utilises hadronic cascade models to describe the gradual freezeout [2, 3, 9, 10, 11] in a more realistic way. As will be shown, the hadronic afterburner is mandatory in understanding elliptic flow data. Phase space distributions for hadrons are initialized below T_c by using the Cooper-Frye formula. We employ a hadronic cascade model JAM [12] to describe the space-time evolution of the interacting hadron gas. This kind of hybrid approaches in which the QGP fluids are followed by hadronic cascade models automatically describes both the chemical and thermal freezeout and is much more realistic especially for the late stage than the naive Cooper-Frye prescription.

Initial conditions in hydrodynamic simulations are so chosen as to reproduce the centrality and rapidity dependences of multiplicity $dN_{\text{ch}}/d\eta$. Initial conditions here are energy density distribution $e(x, y, \eta_s)$ and flow velocity $u^\mu(x, y, \eta_s)$ at the initial time τ_0 . Again baryon density is neglected since the net baryon density is quite small at midrapidity at RHIC. At mid-(space-time)rapidity $\eta_s = 0$, one can parametrise the initial entropy density based on the Glauber model

$$s(x, y) = \frac{dS}{\tau_0 d\eta_s d^2x_\perp} \propto \alpha n_{\text{part}}(x, y; b) + (1-\alpha)n_{\text{coll}}(x, y; b) \quad (2)$$

The soft/hard fraction α is adjusted to reproduce the measured centrality dependence [13] of the charged hadron multiplicity at midrapidity. By using the EoS, one can calculate the initial energy density distribution together with pressure and temperature distributions from Eq. (2). For space-time rapidity dependence of initial conditions and a novel initial condition based on the colour glass condensate (CGC) picture, see Refs. [2, 14]. The fitting of multiplicity is the starting point of further analysis based on hydrodynamic simulations.

In the hydrodynamic models, various combinations of initial conditions, EoS and decoupling prescriptions are available to analyse the experimental data. Of course, final results largely depend on modeling of each stage. So it is quite important to constrain each model and its inherent parameters through systematic analysis of the data toward a comprehensive understanding of the QGP.

3. Elliptic flow

Anisotropic transverse flow can be quantified by Fourier components of azimuthal distribution, $v_n = \langle \cos n\varphi \rangle$, where the average is taken over by weighting azimuthal distribution. The second harmonics v_2 is called elliptic flow parameter and is intimately related with the EoS and the degree of thermalisation [15].

3.1. Charged hadrons

The pseudorapidity dependence of v_2 observed by PHOBOS [16] has a triangular shape: v_2 is maximum at midrapidity and decreases as moving away from midrapidity. On the other hand, in the ideal hydrodynamic calculations with $T^{\text{dec}} = 100$ MeV, v_2 depends

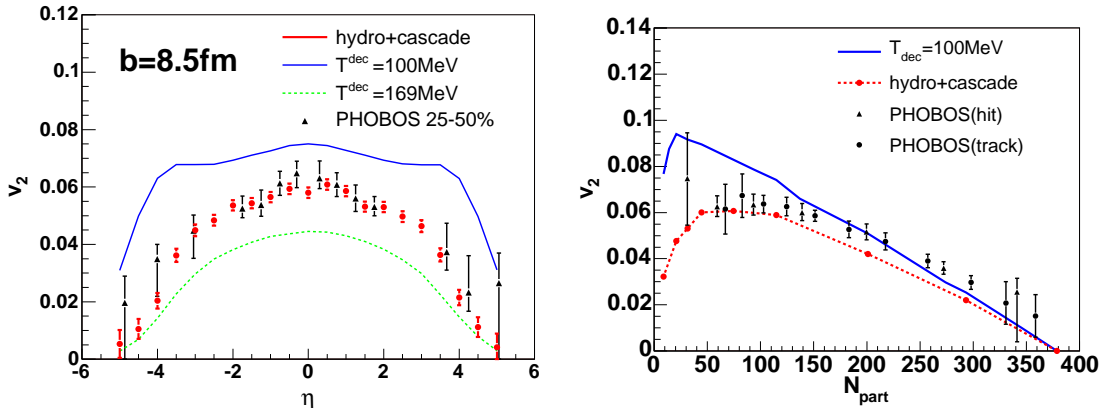


Figure 1. (Left) Pseudorapidity dependence of v_2 for charged hadrons. PHOBOS data [16] are compared to the ideal hydrodynamic model with $T^{\text{dec}} = 100$ and 169 MeV and the hybrid model [2]. (Right) v_2 for charged hadrons as a function of centrality in $|\eta| < 1$. PHOBOS data [16] are compared to the ideal hydrodynamic model with $T^{\text{dec}} = 100$ MeV and the hybrid model [2].

mildly on pseudorapidity in $|\eta| < 3$. Consequently, the hydrodynamic model generates as large v_2 as the data only near midrapidity and overshoots the data significantly at forward and backward rapidities [7, 17] as shown in Fig. 1 (left). If we replace the hadron fluid with a hadron gas utilising a hadronic cascade, v_2 is generated little in the forward and backward region during hadronic rescattering stage [2]. In this hybrid model the hadrons have a finite mean free path and exhibit an effective shear viscosity in the hadron phase. So the dissipative hadronic “corona” effect [18] turns out to be important in understanding the charged hadron v_2 data. Figure 1 (right) shows the centrality dependence of v_2 at midrapidity ($|\eta| < 1$). The solid line is the result from an ideal hydrodynamic calculation, while the dotted line from the hybrid model. It is clear that for peripheral collisions where the multiplicity is small the hadronic viscosity plays an important role in description of the v_2 data. One may notice that the result from the hybrid model systematically and slightly smaller than the data. However, there could exist an effect of initial eccentricity fluctuations which is absent in the present hydrodynamic calculations and could enhance v_2 by $\sim 90\%$ in 0-5% and by $\sim 20\%$ in 50-60% centralities [19]. The deviation between the results and the data may be interpreted quantitatively by this eccentricity fluctuation effect.

3.2. Identified hadrons

The hybrid model also reproduces a mass ordering pattern of v_2 for identified hadrons as a function of p_T near midrapidity [20] (Fig. 2, left) and in forward rapidity region [21]. We consider semi-central collisions (20-30% centrality), choosing impact parameter $b = 7.2$ fm. If one would look at the result just after the hadronisation, the difference between pions and protons would be quite small as shown in Fig. 2 (right). As demonstrated in this figure, at low p_T the pion curve moves up while the proton curve

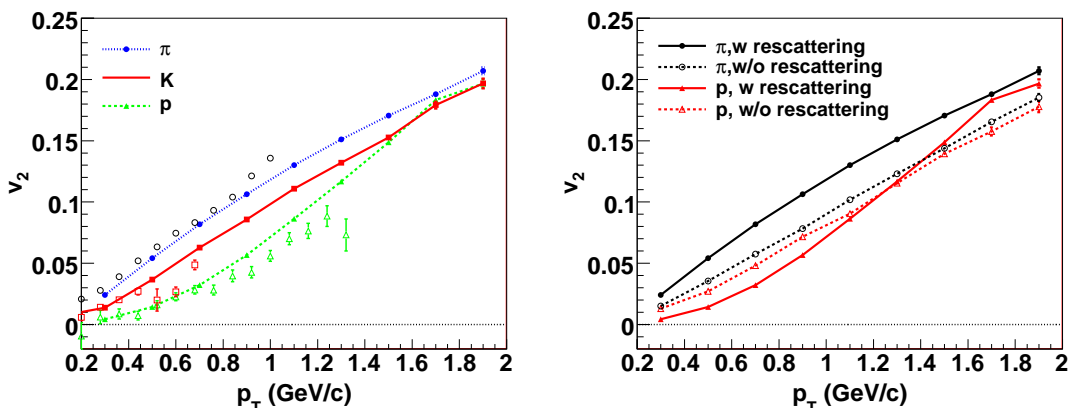


Figure 2. (Left) $v_2(p_T)$ for identified hadrons. STAR data [20] are compared to the hybrid model [3]. (Right) $v_2(p_T)$ with and without hadronic rescattering [3].

moves down through rescatterings. So the hadronic rescatterings are attributed to the observed splitting patterns of $v_2(p_T)$. It should be noted that the same hadronic rescattering effect is also seen in the recent study based on the different hadronic cascade model [22]. One can conclude that the large magnitude of the integrated v_2 and the strong mass ordering of the differential $v_2(p_T)$ observed at RHIC result from a subtle interplay between perfect fluid dynamics of the early QGP stage and dissipative dynamics of the late hadronic stage. The large magnitude of v_2 is due to the large overall momentum anisotropy, generated predominantly in the early QGP stage. Whereas the strong mass splitting behavior at low p_T reflects the redistribution of this momentum anisotropy among the different hadron species during the hadronic rescattering phase.

Hadronic rescattering turns out to cause the mass ordering of $v_2(p_T)$. Then, what happens to the (hidden) strangeness sector in which rescattering with other hadrons does not happen so frequently [23]? Figure 3 (left) shows $v_2(p_T)$ for π , p and ϕ . The $v_2(p_T)$ curves for pions and protons separate as discussed before, whereas $v_2(p_T)$ for the ϕ meson remains almost unchanged during the hadronic stage. As a result of rescattering the proton elliptic flow ends up being smaller than that of the ϕ meson, $v_2^p(p_T) < v_2^\phi(p_T)$ for $0 < p_T < 1.2$ GeV/c, even though $m_\phi > m_p$. Hadronic dissipative effects are seen to be particle specific, depending on their scattering cross sections which couple them to the medium. The large difference of cross section between protons and ϕ mesons in the hadronic rescattering phase leads to a violation of the hydrodynamic mass ordering at low p_T in the final state. Note that clear mass ordering is seen in Fig. 3 (right) if ϕ mesons were also assumed to fully participate in hydrodynamic flow.

4. Application of hydrodynamic results

So far, we have seen that the hybrid model, in which the dynamical evolution of the locally thermalised QGP and the dissipative hadronic gas are incorporated, works well in describing the elliptic flow data. One can utilise the space-time evolution of the QGP

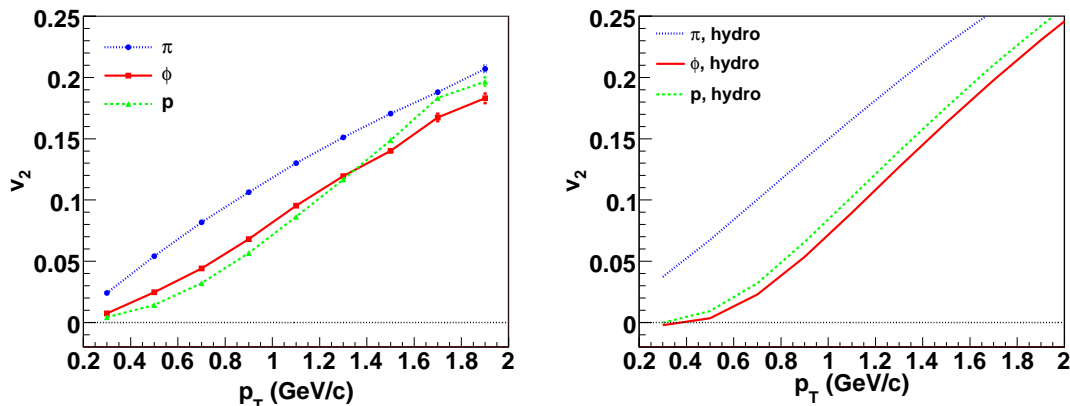


Figure 3. $v_2(p_T)$ for pions (dotted), protons (dashed) and ϕ mesons (solid) in Au+Au collisions at $b = 7.2$ fm from the hybrid model (left) and from the ideal hydrodynamic model with $T^{\text{dec}} = 100$ MeV (right).

obtained above to study other observables.

The charmonium is one of the major diagnostic tools of the QGP in relativistic heavy ion collisions [24]. The melting temperature of J/ψ , ψ' and χ_c is obtained by modeling the free streaming of charmonia on the QGP background [25, 26]. We first generate the charmonia in the transverse plane, distribute them according to the binary collision density, simulate the transverse motion of charmonium and then dissociate them when the temperature at the position of a J/ψ (ψ' and χ_c) is larger than the melting temperature $T_{J/\psi}$ (T_χ). It is found [25, 26] that the suppression pattern as a function of centrality reflects the region of the temperature above $T_{J/\psi}$ which is obtained in hydrodynamic calculations. The best fit to the suppression factor observed by PHENIX [27] is achieved by choosing $T_{J/\psi} = 2T_c$ and $T_\chi = 1.34T_c$.

Thermal photon is one of the direct and penetrating probes to study the QGP [28]. To calculate the transverse momentum spectra of thermal photons, one convolutes the reaction rate, which is the yield per unit space-time volume, over the volume of thermalised matter in heavy ion collisions which is obtained from hydrodynamic simulations. By using the hydrodynamic results obtained in the previous section, we calculate the thermal photon spectra [29, 30] as well as components of hard photons, jet-photon conversion and fragmentation. We find that thermal photons originated from the QGP phase are dominant around $p_T \sim 3$ GeV/c [29, 30].

From hydrodynamic simulations in the previous section, the maximum temperature is found to be at most ~ 400 MeV in central collisions which is much smaller than the mass of heavy quarks. So it is safe to assume that these heavy quarks are not thermally excited and are produced only in the first hard collisions. We treat these heavy particles as ‘‘impurities’’ in the medium in which light degrees of freedom such as u , d and s quarks and gluons are equilibrated. We model the transverse motion of heavy quarks as the Brownian motion and calculate the nuclear modification factor for electrons and positrons from semileptonic decays of heavy mesons and elliptic flow parameter for heavy

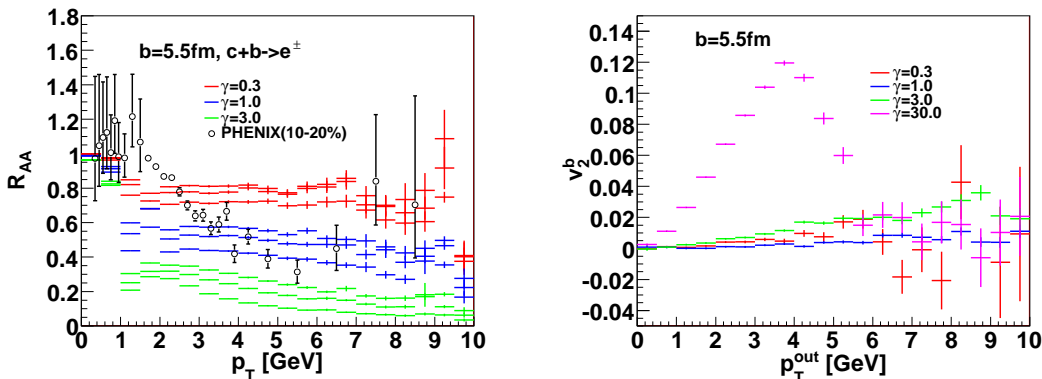


Figure 4. (Left) Nuclear modification factor for electrons and positrons from semileptonic decays in semi-central collisions for $\gamma = 0.3, 1.0$ and 3.0 . Experimental data are obtained by PHENIX [32]. Upper and lower bands represent when diffusion of heavy quarks stops in the mixed phase $f_{\text{QGP}} = 1$ and 0 , respectively, where f_{QGP} is the fraction of the QGP phase in the mixed phase. The middle points in the band correspond to $f_{\text{QGP}} = 0.5$. (Right) Sensitivity of $v_2(p_T)$ for bottom quarks to the parameter in the drag force. Results are obtained with $f_{\text{QGP}} = 0.5$.

quarks. We solve the following relativistic Langevin equations

$$\Delta \vec{x}(t) = \frac{\vec{p}}{E(p)} \Delta t, \quad \Delta \vec{p}(t) = -\Gamma \vec{p} \Delta t + \vec{\xi}(t) \quad (3)$$

on the hydrodynamic background [31]. Here M , \vec{x} and \vec{p} are mass, position and momentum of a sample heavy quark. $\vec{\xi}$ is the Gaussian white noise. We parametrize drag force as $\Gamma = \gamma \frac{T^2}{M}$. The above equations are solved in the local rest frame of a fluid element which is moving with u^μ in the center of mass system. γ in the drag force is the only adjustable parameter in this modeling of heavy quark diffusion. From a comparison of nuclear modification factor with the data in Fig. 4 (left), we find $\gamma \sim 1-3$ gives a reasonable description of the data observed by PHENIX [32]. If we look at $v_2(p_T)$ for heavy quarks just before hadronisation, the results with $\gamma \sim 1-3$ are considerably smaller than the result with $\gamma = 30.0$ whose relaxation time $\tau = 1/\Gamma$ is much smaller than the life time of the QGP. This indicates that the heavy quarks do not reach the complete thermalisation limit.

5. Summary

We discussed the current status of hydrodynamic description of relativistic heavy ion collisions. Integrated and differential elliptic flow parameters in low p_T regions are well reproduced by the hybrid approach in which ideal hydrodynamic description of the QGP is followed by microscopic description of hadron gas. We found the observed mass ordering pattern results from the hadronic rescatterings. As a consequence, violation of mass ordering is predicted for ϕ mesons that do not couple to the hadronic medium. We also discussed the recent application of hydrodynamic results to J/ψ suppression,

thermal photon radiation and heavy quark diffusion.

Acknowledgments

The author would like to thank Y Akamatsu, T Gunji, H Hamagaki, T Hatsuda, U Heinz, D Kharzeev, R Lacey, F M Liu, Y Nara, K Werner and Y Zhu for fruitful discussion. The work was partly supported by Grant-in-Aid for Scientific Research No. 19740130 and by Sumitomo Foundation No. 080734.

References

- [1] Yagi K, Hatsuda T and Miake Y 2005 *Quark-Gluon Plasma* (Cambridge: Cambridge University Press)
- [2] Hirano T, Heinz U W, Kharzeev D, Lacey R and Nara Y 2006 *Phys. Lett. B* **636** 299
- [3] Hirano T, Heinz U W, Kharzeev D, Lacey R and Nara Y, 2008 *Phys. Rev. C* **77** 044909
- [4] Hirano T, van der Kolk N and Bilandzic A 2008 Hydrodynamics and Flow *Preprint* arXiv:0808.2684 [nucl-th].
- [5] Braun-Munzinger P, Redlich K and Stachel J 2003 Particle production in heavy ion collisions *Preprint* arXiv:nucl-th/0304013
- [6] Bebie H, Gerber P, Goity J L and Leutwyler H 1992 *Nucl. Phys. B* **378** 95
- [7] Hirano T and Tsuda K 2002 *Phys. Rev. C* **66** 054905
- [8] Cooper F and Frye G 1974 *Phys. Rev. D* **10** 186
- [9] Bass S A and Dumitru A 2000 *Phys. Rev. C* **61** 064909
- [10] Teaney D, Lauret J and Shuryak E V 2001 *Phys. Rev. Lett.* **86** 4783
- [11] Nonaka C and Bass S A 2007 *Phys. Rev. C* **75** 014902
- [12] Nara Y, Otuka N, Ohnishi A, Niita K and Chiba S 2000 *Phys. Rev. C* **61** 024901
- [13] Back B B *et al* (PHOBOS Collaboration) 2002 *Phys. Rev. C* **65** 061901
- [14] Hirano T and Nara Y 2004 *Nucl. Phys. A* **743** 305
- [15] Ollitrault J Y 1992 *Phys. Rev. D* **46** 229
- [16] Back B B *et al* (PHOBOS Collaboration) 2005 *Phys. Rev. C* **72** 051901
- [17] Hirano T 2002 *Phys. Rev. C* **65** 011901
- [18] Hirano T and Gyulassy M 2006 *Nucl. Phys. A* **769** 71
- [19] Hirano T and Nara Y in preparation
- [20] Adams J *et al* (STAR Collaboration) 2005 *Phys. Rev. C* **72** 014904
- [21] Sanders S J *et al* (BRAHMS Collaboration) 2007 *J. Phys. G: Nucl. Phys.* **34** S1083
- [22] Werner K, these proceedings
- [23] Shor A 1985 *Phys. Rev. Lett.* **54** 1122
- [24] Matsui T and Satz H 1986 *Phys. Lett. B* 178 416
- [25] Gunji T, Hamagaki H, Hatsuda and Hirano T 2007 *Phys. Rev. C* **76** 051901
- [26] Gunji T, these proceedings
- [27] Adare A *et al* (PHENIX Collaboration) 2007 *Phys. Rev. Lett.* **98** 232301
- [28] Shuryak E 1978 *Phys. Lett. B* **78** 150
- [29] Liu F M, Hirano T, Werner K and Zhu Y 2008 Centrality-dependent direct photon p_t spectra in Au + Au collisions at RHIC *Preprint* arXiv:0807.4771 [hep-ph]
- [30] Liu F M, these proceedings
- [31] Akamatsu Y, Hatsuda T and Hirano T 2008 Heavy Quark Diffusion with Relativistic Langevin Dynamics in the Quark-Gluon Fluid *Preprint* arXiv:0809.1499 [hep-ph]
- [32] Adare A *et al* (PHENIX Collaboration) 2007 *Phys. Rev. Lett.* **98** 172301